

# Measurement of Mutual Coulomb Dissociation in $\sqrt{s_{NN}} = 130$ GeV Au+Au collisions at RHIC

Mickey Chiu<sup>a</sup>, Alexei Denisov<sup>b</sup>, Edmundo Garcia<sup>c,\*</sup>, Judith Katzy<sup>d</sup>, Andrei Makeev<sup>e</sup>, Michael Murray<sup>e</sup> and Sebastian White<sup>f</sup>

<sup>a</sup> Columbia University, New York, NY 10027

<sup>b</sup> IHEP, Protvino, Russia

<sup>c</sup> U. of Maryland, College Park, Md 20742

<sup>d</sup> MIT, Cambridge, MA 02139

<sup>e</sup> Texas A&M Univ, College Station, TX 77843

<sup>f</sup> Brookhaven National Laboratory, Upton, NY 11973-5000

## Abstract

We report on the first measurement of Mutual Coulomb Dissociation in heavy ion collisions. We employ forward calorimeters to measure neutron multiplicity at beam rapidity in peripheral collisions. The cross-section for simultaneous electromagnetic breakup of Au nuclei at  $\sqrt{s_{NN}} = 130$  GeV is  $\sigma_{MCD} = 3.67 \pm 0.25$  barns in good agreement with calculations.

PACS numbers: 25.75.-q, 29.27.-a, 29.40.Vj, 25.20.-x

An interesting aspect of the Relativistic Heavy Ion Collider(RHIC) is the high rate of  $\gamma - \gamma$  and  $\gamma$ -hadron collisions it produces. For example, under nominal running conditions, with colliding gold beams, the  $\gamma$ -nucleus luminosity is  $\sim 10^{29} cm^{-2} \cdot s^{-1}$  for equivalent photon energies with  $2 \text{ GeV} \leq E_\gamma \lesssim 300 \text{ GeV}$ . The process of electromagnetic dissociation is a well-known feature of heavy ion collisions. For those collisions where the impact parameter is larger than the sum of the nuclear radii, one nucleus may, nevertheless, undergo interaction with the intense electric field of the other nucleus. This process is described in terms of the Weizsäcker-Williams formalism and is typically dominated by the large photonuclear cross-section at the Giant Dipole Resonance from equivalent photons with energy,  $E_\gamma < 24 \text{ MeV}$ .

The cross-section for the above reaction (“single beam dissociation”) is quite large [1] (95 barns for  $\sqrt{s_{NN}} = 200 \text{ GeV}$  Au beams) and limits the maximum beam lifetime at RHIC. In this paper we report on the first measurement of Mutual Coulomb Dissociation (MCD) whereby both beam nuclei dissociate electromagnetically. This process was first studied because of its potential use for luminosity monitoring at RHIC [2,3]. Calculations [4,5] have shown that it is dominated by second order 2-photon exchange and results in emission of a few neutrons with small (few MeV) kinetic energy in the nucleus rest frame. The current paper deals with dissociation of Au ions with energy of 65 GeV/nucleon so these neutrons have small angular and energy spread with respect to the beam.

The present work is based on data at 3 RHIC interaction regions - at the PHENIX, BRAHMS and PHOBOS [6] locations. Experimentally, we measure the multiplicity of emitted neutrons along each beam direction with Zero Degree Calorimeters(ZDCs) [8] and determine the relative topological cross-sections  $Au + Au \rightarrow N_{neutrons}^{Left} + N_{neutrons}^{Right} + X + Y$ , where neutron multiplicities are specified but we sum over all possible emission of protons and gamma rays, for example. Specific channels are calculated in Refs. [4,5] and we compare to these predictions.

In addition to measuring beam fragmentation neutrons, the experiments recorded hits in beam-beam counters, which indicated particle production in the central region, hence a nuclear collision. We use the beam-beam counter tag of nuclear inelastic collisions to measure the ratio of Coulomb to nuclear inelastic cross-sections.

The ZDCs are a triggering device used in all of the RHIC experiments. They are small transverse-area hadron calorimeters which measure the energy of unbound neutrons in small forward cones around each beam ( $|\theta| < 2 \text{ mrad}$ ). The layout of the ZDCs is shown in Fig. 1 and further details can be found in Ref. [8]. The ZDC interaction trigger required a coincidence between ZDCs on either side of the interaction region (referred to as ZDC left, right) where a hardware threshold equivalent to 12 GeV was applied to the signal. The ZDC energy scale was determined from the one neutron and two neutron peaks which are clearly seen in Fig. 3. The energy resolution for 65 GeV neutrons was approximately 21% consistent with earlier test beam results [8].

In addition, PHENIX used a set of Beam-Beam Counters(BBC’s) [9] on which we base the following discussion (the BRAHMS and PHOBOS results presented in this paper were obtained from similar analyses based on BBC arrays with different pseudo-rapidity coverage) [6,7]. The PHENIX BBC’s are arrays of quartz Cerenkov detectors which measure relativistic charged particles produced in cones around each beam ( $3.05 < |\eta| < 3.85$ , with  $2\pi$  azimuthal coverage). There are 64 photomultiplier (PMT) channels in each BBC arm. A BBC coincidence required more than 1 hit above a preset threshold ( $n_{BBC} > 1$ ) in each

arm. An event vertex requirement was also applied to ZDC trigger events ( $|z| \leq 20$  cm) where the vertex location was calculated using the time-of-flight to the ZDCs. This event selection is identical to the selection used in Ref. [9] and the vertex position obtained with the ZDC and BBC detectors was identical within a resolution of  $\leq 2$  cms. A total of 160,601 ZDC trigger events satisfied these requirements.

The BBC coincidence was used in the present analysis to tag hadronic collisions for those events which trigger the ZDCs. In addition, PHENIX recorded several million events triggered with the BBC coincidence alone. These events were used to estimate the ZDC trigger efficiency for hadronic collisions.

In Fig. 2 we plot the neutron multiplicity measured in the ZDCs versus the BBC multiplicity (i.e. integrated charge) normalized to a full scale total charged multiplicity of 1,000 in the angular interval covered by these detectors [10]. For the purposes of this paper we identify 2 classes of events according to the number of hit BBC PMTs.

1. Inelastic “Hadronic” events for which  $n_{BBC} > 1$  in each arm.
2. Peripheral, “Coulomb” events for which  $n_{BBC} \leq 1$  in at least one arm.

The fraction of events which satisfy the BBC requirement for Coulomb and hadronic collisions was derived from simulations of particle production in the 2 types of events. In Coulomb interactions, since most of the cross-section is due to equivalent photons with energy below particle production threshold, essentially all events satisfy the “Coulomb” event selection. In fact, the fraction of Coulomb interactions with a produced  $\pi^\pm$  resulting in at least one BBC hit is found to be  $\sim 3\%$  [5] so vetoing on the coincidence introduces an inefficiency of  $\leq 1\%$ . On the other hand,  $8 \pm 2\%$  of hadronic interactions [9,11] are estimated to fail the “Hadronic” BBC cut and these events represent a 14% contamination of the “Coulomb” sample.

The “Hadronic” BBC cut mis-identification is caused by peripheral hadronic events corresponding to a few elementary N-N collisions so low multiplicity BBC events were used to model the background in the “Coulomb” sample. Diffractive hadronic interactions are not treated in our particle production simulation and these are a potential background to our “Coulomb” sample. However this is a negligible correction since, for example, the high energy p-W diffraction dissociation cross-section [12] is 20 mb -which is a small fraction of the total p-W inelastic cross-section.

The ZDC multiplicity spectra are very different for the 2 classes of events as can be seen from Fig. 3; the “Coulomb” events tend to have low total neutron multiplicity whereas the fraction of “Hadronic” events with 1 or 2 neutrons is very small. The background (to the Coulomb) shape was calculated using low multiplicity tagged “Hadronic” events as described above and applied as a correction in what follows. As a check on consistency of this subtraction procedure, an un-normalized Coulomb ZDC multiplicity spectrum was obtained by measuring the left ZDC distribution with a 1 neutron cut on the multiplicity in the right one. This cut strongly suppresses nuclear collisions. This shape was then renormalized and subtracted from the raw “Coulomb” distribution. The background shape so obtained is identical within errors to that shown in Fig. 3.

The ZDC trigger efficiency correction was obtained from the geometrical acceptance for neutrons in the ZDC. The angular distribution of neutrons about the beam direction is

expected to be very different for hadronic and Coulomb events so we discuss these 2 cases separately. Angular distributions and spectra of neutrons from low energy photoproduction experiments [13,14] were used to compute the angular spread of Coulomb Dissociation neutrons about the beam direction. The maximum  $p_t$  was 120 MeV so the maximum opening angle was less than 2 mrad. In the photoproduction experiments, the average neutron multiplicity was found to increase with photon energy. Comparable spectra for high energy photoabsorption are not available (note that  $\sim 20\%$  of the MCD cross section is due to equivalent photons with energy  $\geq 2$  GeV) however we can safely assume that the mean neutron multiplicity is larger than 1 based on the lower energy data. Therefore, no ZDC acceptance correction is applied to the measured Coulomb rates.

The ZDC acceptance correction for hadronic collisions was both calculated using the  $p_t$  spectrum characteristic of a Fermi distribution [15] and measured using the independent BBC trigger sample. The calculated geometrical acceptance per neutron in the ZDC detector is 75% at  $\sqrt{s_{NN}}=130$  GeV/c. As can be seen from Fig. 2, multiple neutrons are detected for most nuclear collisions, therefore the ZDC detection efficiency per event is close to unity. From this acceptance and the observed spectrum of “Hadronic” events in Fig. 3 we estimated the losses due to the ZDC requirement and found excellent agreement with the measured trigger efficiency.

To directly measure the ZDC trigger efficiency we scanned the BBC trigger events for interactions in which the ZDC trigger condition failed. The measured efficiency is  $98 \pm 2\%$  and this correction is applied to the calculated hadronic rates.

The cross-sections derived in this paper are as ratios relative to the ZDC total cross section. The latter was calculated to be 10.8 barns [4] at  $\sqrt{s_{NN}} = 130$  GeV ( and 11.0 barns at  $\sqrt{s_{NN}} = 200$  GeV) with a theoretical uncertainty of less than  $\pm 5\%$ .

In order to determine  $\sigma_{MCD}$  we correct our measured ratio of “Hadronic” events ( $N_{Hadronic}$ ) to total events ( $N_{Total}$ ) for the (experiment dependent) BBC trigger efficiency,  $\epsilon_{BBC}$ . Thus

$$\sigma_{MCD} = \sigma_{tot} - \sigma_{geom} = \sigma_{tot} \cdot \left(1 - \frac{1}{\epsilon_{BBC}} \cdot \frac{N_{Hadronic}}{N_{Total}}\right) \quad (0.1)$$

and the error on  $\sigma_{MCD}$  has contributions from the measured ratios, the experimental BBC efficiency and the theoretical error on  $\sigma_{tot}$ . The PHENIX BBC trigger efficiency was found to be  $[92 \pm 2(syst)]\%$  of the nuclear interaction cross-section (i.e.  $\sigma_{geom}$ ), with a background contamination of  $[1 \pm 1(syst)]\%$  [9,11]. The trigger efficiency is, as it turns out, very weakly dependent on input assumptions of the Glauber model, such as the radius parameter. Note that it is only this efficiency and not the Glauber cross-section that is used in the current analysis.

Table 1 presents our measured value of the ratio of  $\sigma_{geom}$  to the total ZDC cross section, which is in good agreement with the ratio calculated in both refs. [4,5]. The ratio of “Hadronic” to “Hadronic” + “Coulomb”, as defined above, is corrected for BBC efficiency.

To compare to specific channels calculated for Mutual Coulomb Dissociation, we fit the measured ZDC energy spectra to neutron multiplicity distributions, taking into account the experimental resolution of the ZDCs. We constrained the fits such that  $\sigma_E(2n) = \sqrt{2} \times \sigma_E(1n)$ , etc. Fig. 3 shows the energy spectrum obtained in one ZDC (ZDC left) for the “Coulomb” event selection when the other ZDC pulse height is consistent with 1 neutron.

The distribution is fit to a linear sum of expected 1 neutron + 2 neutron, etc. energy distributions.

The total number of events in Fig. 3, after background subtraction, corresponds to the cross-section for the (1n,Xn) topology in which one neutron is observed in the right beam direction. We report, in Table 1, the sum of 1 neutron in left and right topologies as (1n,Xn). The fraction of events in the 1 neutron peak measures directly the number of (1n,Xn) with the decay topology (1n,1n), i.e. with exactly 1 neutron in both ZDC left and right. Of course, any number of protons could also be emitted in the reaction but these are not detected. Photons which hit the ZDCs would also contribute to the total energy measured. Details on the photon response may be found in Ref. [8].

Similarly the fits to specific neutron multiplicities in the ZDCs such as (2n,1n) are derived from simultaneous fits to ZDC left, cut on ZDC right, pulse height. The errors indicated include both statistical and systematic errors in the fit procedure. The dominant systematic error comes from sensitivity to the fitted lineshape. The dependence of the lineshape on the neutron multiplicity (i.e. that it grows as  $\sqrt{N_{neutron}}$ ) is justifiable from first principles. However the fitted areas can vary significantly if this constraint on the relative peak widths is removed and this variation is used to derive the systematic errors quoted in Table 1.

In Fig. 4 we compare our measured 2 neutron to 1 neutron ratio to lower energy data [16] on single beam dissociation. There is an apparent trend for this ratio to increase with center of mass energy. Both sets of data are in reasonable agreement with calculated values found in [4,5].

In Coulomb events each nucleus interacts independently with the field of the other. We therefore expect only a weak correlation between fragment multiplicity of the left and right going nuclei. However for nuclear collisions both nuclei have the same number of “wounded nucleons” and therefore the left and right spectra should be correlated, leading to smaller asymmetry:

$$A(E_{Left}, E_{Right}) \equiv \frac{E_{Left} - E_{Right}}{E_{Left} + E_{Right}} \quad (0.2)$$

where  $E_{Left}$  and  $E_{Right}$  are the total ZDC energy signal in the Left and Right ZDCs respectively. For the Coulomb distribution in Fig. 5 we require  $> 1.5$  neutrons energy equivalent in at least 1 of the ZDCs. This suppresses the (1n,1n) events which heavily skew the correlation function. The Coulomb distribution is also corrected for hadronic background.

We observe a class of events in Au+Au collisions at RHIC with low central particle production and a low multiplicity of neutrons at beam rapidity. The cross-section, when compared with the geometrical nuclear cross section is large and in good agreement with earlier calculations of Mutual Coulomb Dissociation. Other features such as the neutron multiplicity distributions are also reasonably well reproduced.

We thank the staff of the RHIC project (particularly A.Drees) and of the Collider-Accelerator and Physics Departments at BNL. We also thank our colleagues on PHENIX, BRAHMS, PHOBOS and the ZDC projects. We thank Tony Baltz and Igor Pshenichnov for numerous useful discussions. We acknowledge support from the US Department of Energy and the Deutsche Forschungsgemeinschaft.

## REFERENCES

- \* present address Univ. of Illinois, Chicago.
- [1] A. J. Baltz, M. J. Rhoades-Brown, J. Weneser, Phys. Rev. E **54**, 4233 (1996).
  - [2] A. J. Baltz, S. N. White, RHIC/DET Note 20, BNL-67127 (1996)
  - [3] S. N. White, Nucl. Instrum. Meth. **A409**, 618 (1998).
  - [4] A. J. Baltz, C. Chasman and S. N. White, Nucl. Instrum. Meth. **A417**, 1 (1998).
  - [5] I. A. Pshenichnov , J. P. Bondorf , I. N. Mishustin , A. Ventura , and S. Masetti, Phys.Rev. C **64**, 024903 (2001) and I.Pshenichnov, private comm.
  - [6] Papers by A.Denisov, J.Katzy and S.N.White , proceedings of the Quark Matter Conference 2001, Nuc. Phys. **A698**, 551c ,555c and 420c (2002).
  - [7] I. G. Bearden *et al.* BRAHMS Collaboration nucl-ex/0108015 accepted by Phys. Lett. B.
  - [8] C. Adler, A. Denisov, E. Garcia, M. Murray , H. Strobele and S. White Nucl. Instrum. Meth. A **470**, 488(2001).
  - [9] PHENIX Collaboration, K. Adcox, *et al.*, Phys. Rev. Letters **86**(2001).
  - [10] Note that this distribution differs somewhat from the corresponding one in ref [9], where the BBC phototubes were run at high gain for timing purposes but suffered some pulse height saturation.
  - [11] The cross-section was calculated using a Glauber model with a Woods-Saxon distribution with radius,  $R=6.65 \pm 0.3\text{fm}$ , diffusivity  $a_0 = 0.54 \pm 0.01\text{fm}$  and a nucleon-nucleon inelastic cross section  $\sigma_{nn} = 40 \pm 5\text{mb}$ . See also C.J.Batty, E.Friedman, A.Gal, Progr. Theor. Phys. Suppl. **117**, 227 (1994).
  - [12] T. Akesson et al. Z.Phys. C **49**, 355-366 (1991)
  - [13] F. Tagliabue, J. Goldemberg, Nucl.Phys. **23**, 144(1961).
  - [14] A. Veyssiere et al. Nucl. Phys. **A159**, 561(1970)
  - [15] see J.Barette et al. Phys. Rev. C **45**, 819(1992), and references therein.
  - [16] T.Aumann et al., Phys.Rev.C **47**, 1728 (1993) and proceedings of the Heavy Ions at the AGS meeting, 1996, p. 286.

# FIGURES

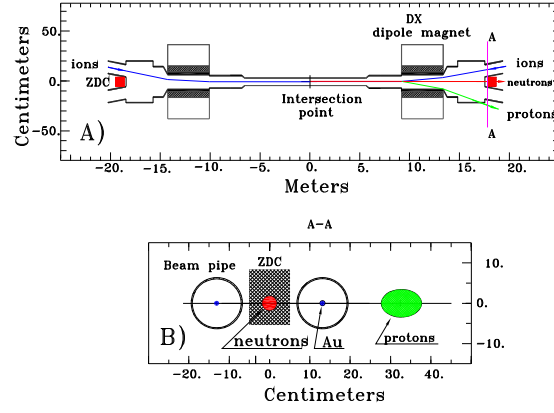


FIG. 1. ZDC location in the RHIC experiments.

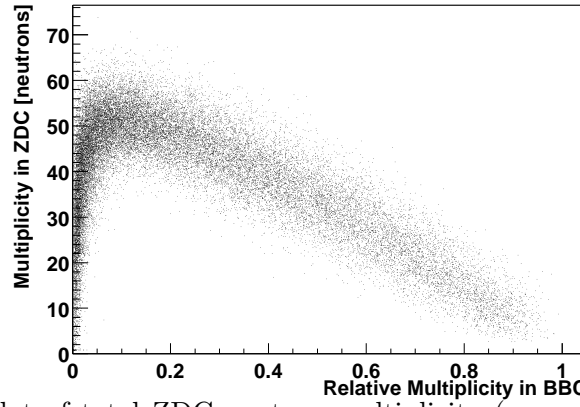


FIG. 2. Scatter plot of total ZDC neutron multiplicity (sum of 2 arms) versus the relative BBC hit multiplicity.

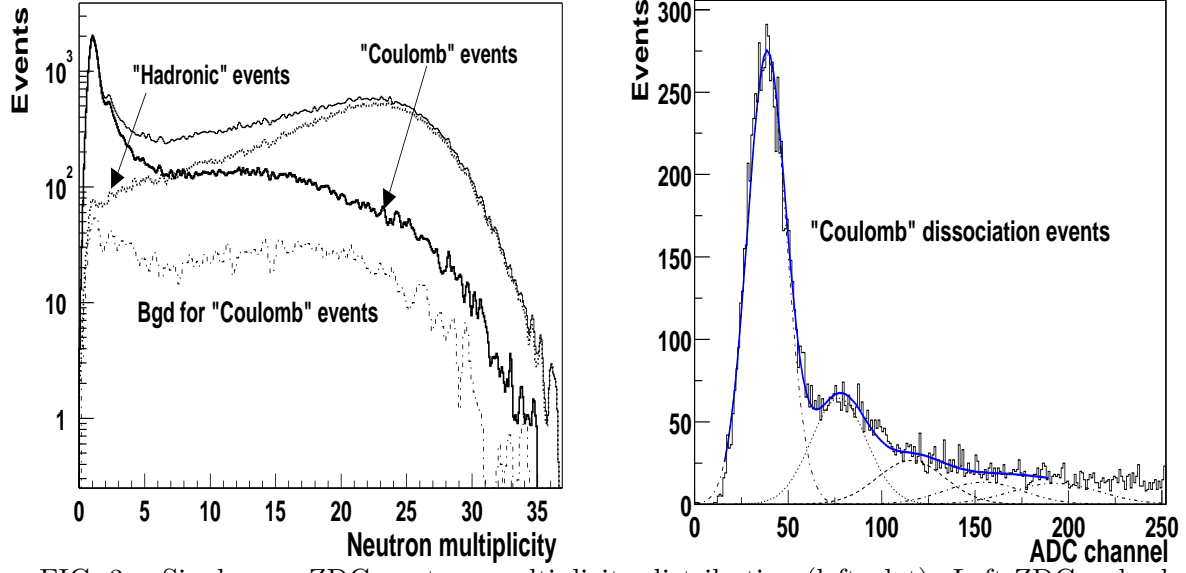


FIG. 3. Single arm ZDC neutron multiplicity distribution (left plot). Left ZDC pulse height with “Coulomb” selection when Right ZDC pulse height is selected to be within the 1n peak (right plot).

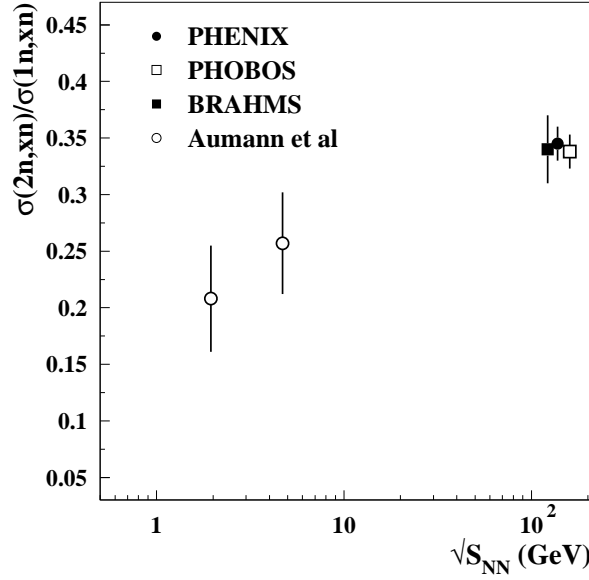


FIG. 4. Ratio of 2n to 1n cross-sections vs. center of mass energy.



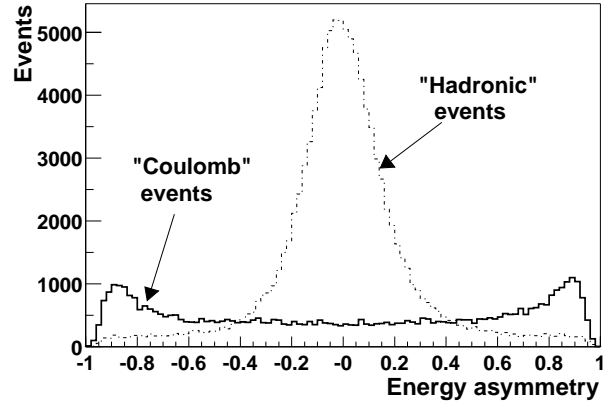


FIG. 5. ZDC asymmetry distributions for Coulomb and nuclear events.

# TABLES

$\sigma_i$ (barns)	Theory [4]	Theory [5]	PHENIX	PHOBOS	BRAHMS
$\sigma_{tot}$	$10.8 \pm 0.5$	11.19	N.A.	N.A.	N.A.
$\sigma_{geom}$	7.09	7.29	N.A.	N.A.	N.A.
$\frac{\sigma_{geom}}{\sigma_{tot}}$	0.67	0.659	$0.661 \pm 0.014$	$0.658 \pm 0.028$	$0.68 \pm 0.06$
Coulomb					
$\frac{\sigma(1n,Xn)}{\sigma_{tot}}$	0.125	0.139	$0.117 \pm 0.004$	$0.123 \pm 0.011$	$0.121 \pm 0.009$
$\frac{\sigma(1n,1n)}{\sigma(1n,Xn)}$	0.329	–	$0.345 \pm 0.012$	$0.341 \pm 0.015$	$0.36 \pm 0.02$
$\frac{\sigma(2n,Xn)}{\sigma(1n,Xn)}$	–	0.327	$0.345 \pm 0.014$	$0.337 \pm 0.015$	$0.35 \pm 0.03$